

Supplementary Information

Conformal N-doped carbon on nanoporous TiO₂ spheres as a high-performance anode material for lithium-ion batteries

Yun Qiao, Xianluo Hu,* Yang Liu, Chaoji Chen, Henghui Xu, Dongfang Hou, Pei Hu, and Yunhui Huang*

State Key Laboratory of Material Processing and Die & Mould Technology, School of Materials Science and Engineering, Huazhong University of Science and Technology, Wuhan 430074, P. R. China.

* Corresponding author

E-mail: huxl@mail.hust.edu.cn; huangyh@mail.hust.edu.cn.

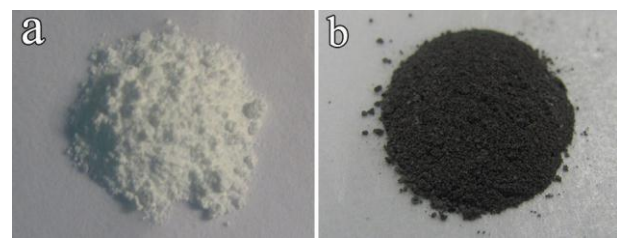


Fig. S1 Digital photos for the powder samples. (a) nanoporous TiO_2 spheres; (b) $\text{TiO}_2@\text{NC}$ nanocomposite.

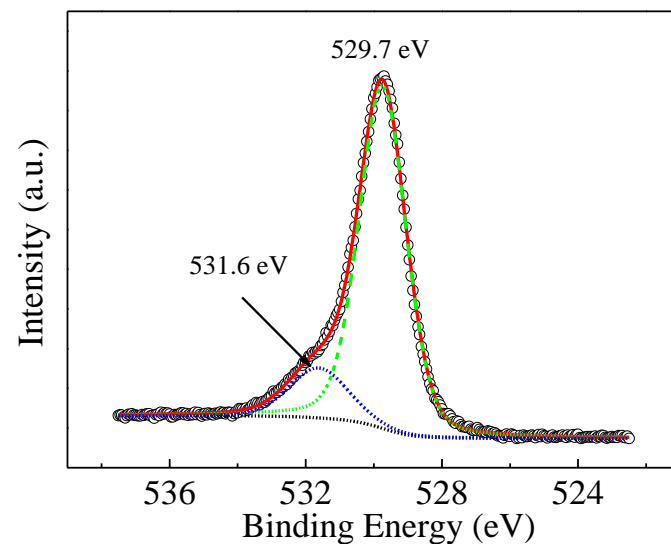


Fig. S2 High-resolution XPS O 1s spectra for the $\text{TiO}_2@\text{NC}$ nanocomposite.

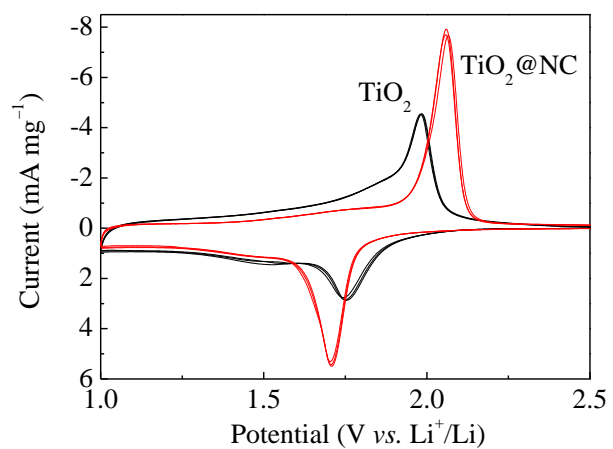


Fig. S3 CV curves for the nanoporous TiO_2 spheres and the $\text{TiO}_2@\text{NC}$ nanocomposite at a scan rate of 0.2 mV s^{-1} (from the second to the forth).

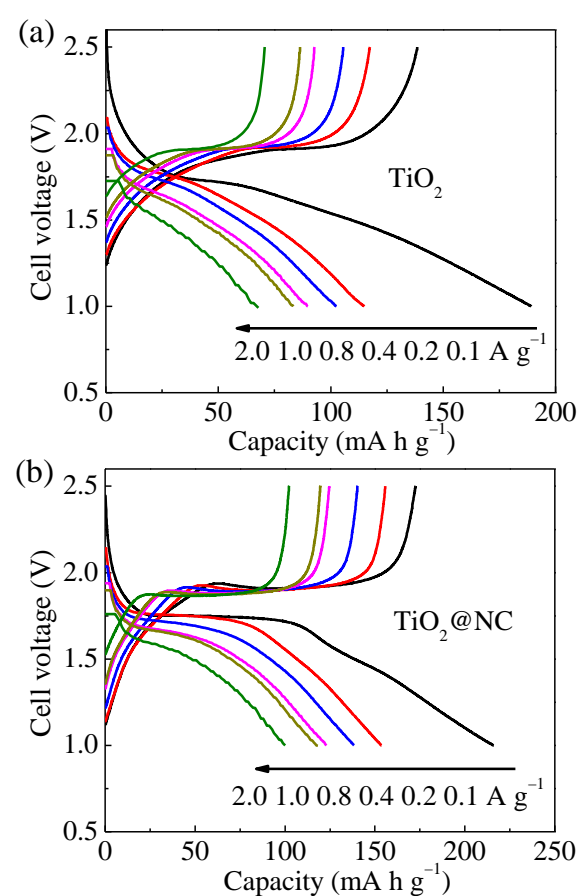


Fig. S4 Charge and discharge curves for (a) the nanoporous TiO₂ spheres and (b) the TiO₂@NC nanocomposite at current densities varying from 0.1 to 2.0 A g⁻¹ each for 10 cycles.

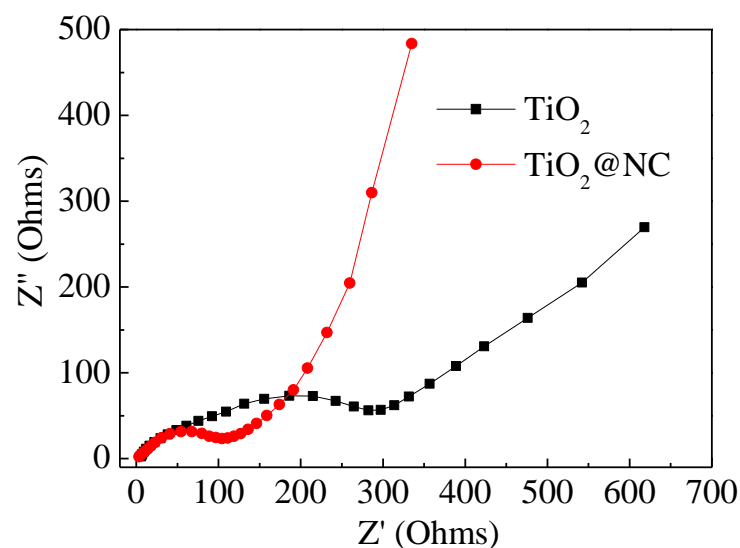


Fig. S5 Electrochemical impedance spectra of the electrodes made of the pure porous TiO_2 nanospheres and the as-formed $\text{TiO}_2@\text{NC}$ hybrid.

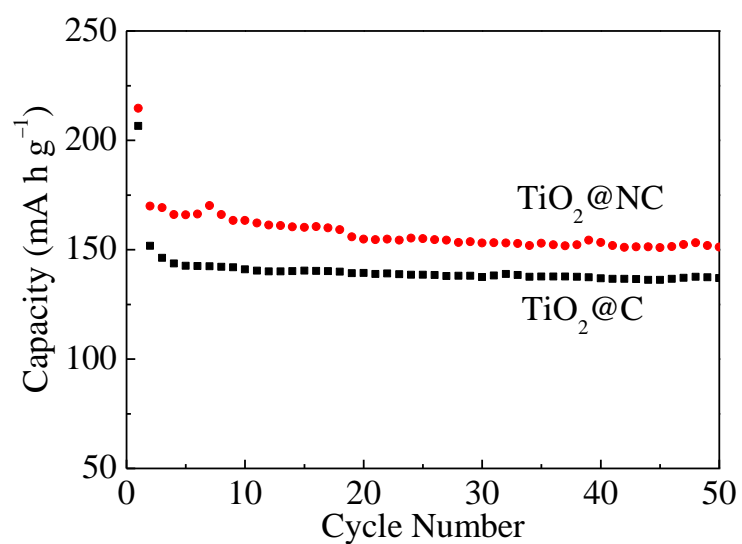


Fig. S6 Cycling performance of the TiO₂@C and TiO₂@NC electrodes at a current density of 100 mA g⁻¹.

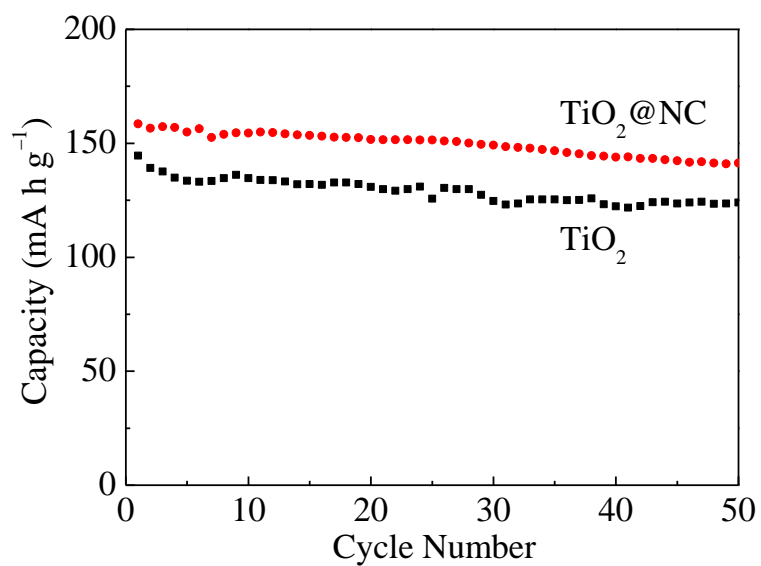


Fig. S7 Cycling performances of the nanoporous TiO₂ spheres and the TiO₂@NC nanocomposite after rate

performance shown in Fig.7c.

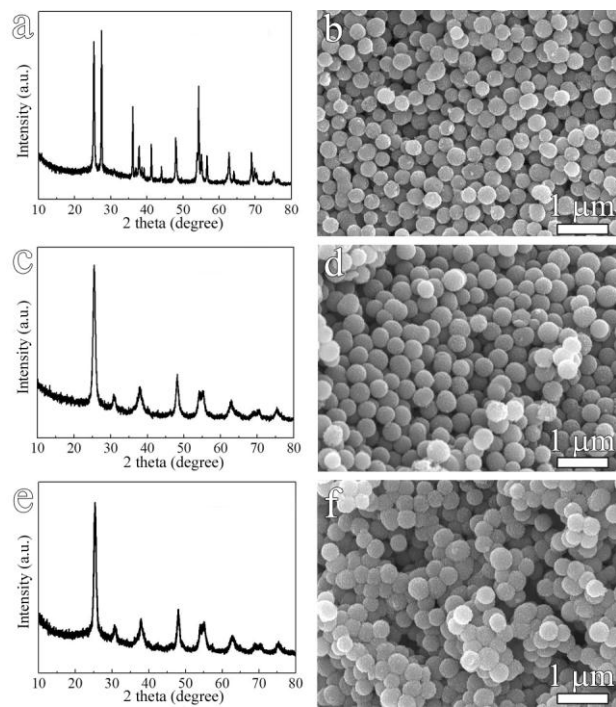


Fig. S8 XRD patterns and FESEM images of TiO₂@NC-0 (a and b),
TiO₂@NC-1 (c and d), TiO₂@NC-3 (e and f).

The TiO₂@NC-0 sample without ILs is composed of anatase and rutile, the high intensity of rutile indicates its content is not just a little. However, the XRD patterns of TiO₂@NC-1 and TiO₂@NC-3 with different amount of ILs are consistent with the TiO₂@NC-2 and nanoporous TiO₂ spheres. It demonstrates that the addition of ILs had a great effect on restraining the transformation to rutile from anatase. The morphology of TiO₂@NC-3 is relatively agglomerated than the other samples, because the adsorption ability of nanoporous TiO₂ spheres reaches the super-saturation state.

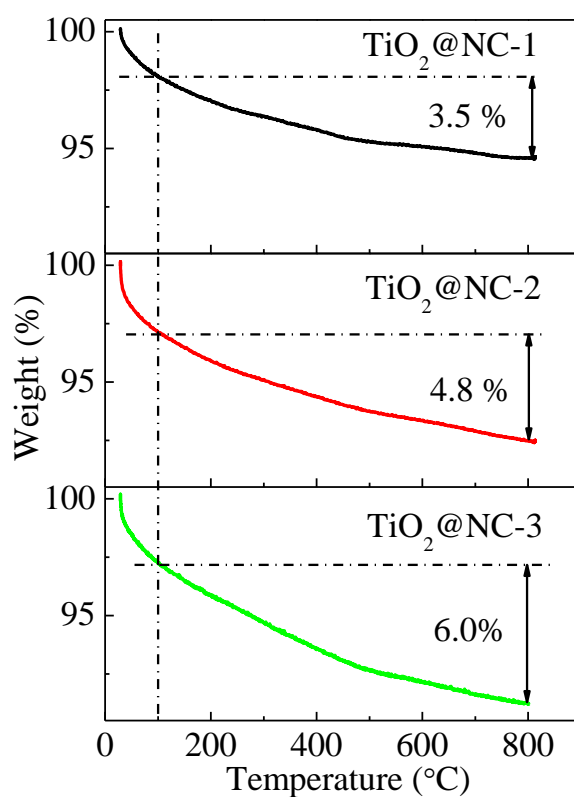


Fig. S9 TG curves of the TiO₂@NC nanocomposites at a heating rate of 10 °C min⁻¹ in flowing air. The large weight loss below 400 °C in TG curves corresponds to the removal of absorbed water from the sample and the decomposition of partial carbon.

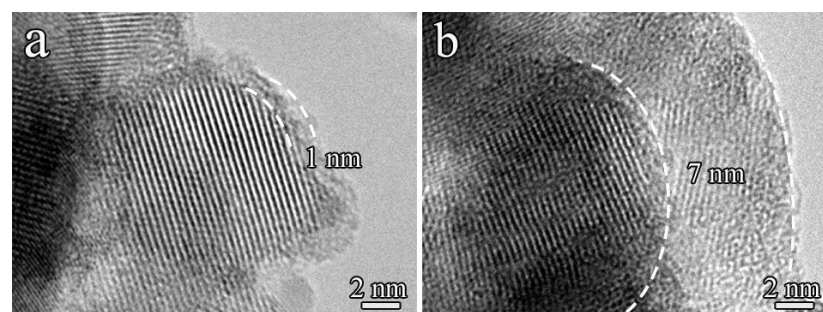


Fig. S10 HRTEM images for (a) the $\text{TiO}_2@\text{NC-1}$ composite and (b) the $\text{TiO}_2@\text{NC-3}$ composite.